MODELLING OF COMPOSITE REPAIRS FOR STEEL PRESSURE PIPING

J.M. Linden[1,3], M. Köpple[2,3], D. Elder[2,3], A.G. Gibson[1*]

[1]*Centre for Composite Materials Engineering, School of Mechanical & Systems Engineering, Newcastle University, Stephenson Bldg, Claremont Rd., NE1 7RU, Newcastle upon Tyne, UK*
[2]*Advanced Composite Structures Australia Pty Ltd, 4/11 Sabre Drive, Port Melbourne, Victoria, 3207, Australia*
[3]*Cooperative Research Centre for Advanced Composite Structures, 506 Lorimer Street, Fishermans Bend, Victoria, 3207, Australia*
**a.g.gibson@ncl.ac.uk*

Keywords: blister test, fracture mechanics, composite repair, crack opening

Abstract

Increasing use of composite repairs in the oil and gas industry brings up the need to develop standards for reliable and cost-efficient design. ASME and ISO published standards. This work points out inaccuracies in results of the energy release rate of the blister "blow-off" test between the analytical model, offered by the standards, and finite element analysis (FEA) simulations. Corrections for the formulations emerged out of this work and showed good agreement with the FEA.

1 Introduction

The use of composite materials for repair and rehabilitation of pipelines and structures has increased over the past decades, especially in the highly corrosive environments that can be found in the production of oil and gas. The advantages of composite over metallic repairs or a full replacement of pipe sections included a better corrosion resistance, higher flexibility for the repair of complex structures, no production shut down or hot work and a minimal lead time. Composite repairs can be divided in two main groups: pre-cured and wet laminates. The biggest advantage of wet laminates over pre-cured is the flexibility to be applied to complex geometries such as bends in pipes or other steel structures of vessels and rigs. Wet laminates are applied uncured in the form of prepreg, by wet lay-up or in some cases using a resin infusion process. Resins used for wet laminates are typically epoxy resins, which are conventional amine cured. In some cases underwater and ultraviolet (UV) cured systems are used as well as vinyl ester and urethane resins. The reinforcing material generally used includes E-glass and carbon, while aramid fibres are used in some cases.

Many new and improved composite repairs have been introduced over the last couple of years. A brief overview of commercially available composite repairs is presented in Table 1. This growth has boosted the need for design standards, which have been developed [1] [2]. One of the main failure modes is delamination in between layers or in the laminate/substrate interface after the fluid has breached through the pipe wall and formed a blister. Therefore one of the main methods of characterisation of a repair system is the blister "blow-off" test [3]. Measuring the failure fluid pressure of the blister allows the calculation of the fracture energy release rate, G_c. An improved version of the analytical model, which can be found in [1] [2], takes into account the bending and shear deflection as well as an additional term for the crack opening displacement. However the analytical results showed to be smaller than those calculated via finite element analysis (FEA).

This paper reports a study to validate and improve the analytical model by utilizing FEA. While the standard only takes quasi-isotropic axi-symmetric models into account, the numerical evaluation allows the consideration of different ply-architectures and substrate defects. The differences between those results are discussed in this paper and used to modify and improve the analytical model.

ClockSpring®	PowerSleeve®	PermaWrap™
ClockSpring® Contour	StrongBack	METALCLAD DuraWrap™
Sitejacket™ Steel	IMG Composites	Carbon Hardshell™
Armor Plate®	DiamondWrap®	Viper-Skin™
A+ Wrap™	Stop It®	Stop It HP™
Furmanite	Aquawrap®	Pipe Wrap
Bolder Wrap	Syntho-Glass® XT	HydraWrap®
PIPEASSURE™	WTR Technowrap	Fortec
Stoptec	Helicoid epoxy sleeve™	

Table 1. Commercial repair systems (non-graded list)

2 Analytical fracture mechanics model

A measure for the quality of a repair-substrate bond is the fracture toughness, K, or the energy release rate, G. Both are connected through the E- and G-modulus as shown in Equation (2) [4]. In the case of plane strain E is divided by $\left(1-\nu_{12}^2\right) \Rightarrow E' = E/\left(1-\nu_{12}^2\right)$. Three different modes of failure can occur: (I) vertical opening, (II) in-plane shear, (III) out-of-plane shear. When $G \geq G_{crit}$, the part will fail through rapid crack propagation.

$$G = \frac{1}{E'}\left(K_I^2 + K_{II}^2\right) + \frac{1}{2G}K_{III}^2 \tag{2}$$

Simplifying the complexity of a corroding pipe wall, the theoretical model for the analytical solution is based on a quasi-isotropic repair laminate on top of a substrate with an artificial corrosion defect (Fig. 1). The analytical model takes into account only cylindrical through hole defects with a sharp rectangular edge at the interface to the repair. In order to be able to calculate the fracture toughness or energy release rate, only the failure pressure has to be measured. Equation (3) shows the derivation of the volume compliance, which leads in conjunction with the pressure to the energy release rate. Accordingly derives the solution for the calculation of the volume in Equation (4).

$$G = \frac{1}{4\pi r}P^2\frac{dC}{dr} = P^2\left(\underbrace{\frac{3\left(1-\nu_{12}^2\right)}{32E_1t^3}r^4}_{Bending} + \underbrace{\frac{3}{20G_{13}t}r^2}_{Shear} + \underbrace{\frac{2\left(1-\nu_{13}\nu_{31}\right)}{\pi E_3}r}_{COD}\right) \tag{3}$$

$$V = 2\pi P\left(\frac{\left(1-\nu_{12}^2\right)}{32E_1t^3}r^6 + \frac{3}{40G_{13}}r^4 + \frac{4\left(1-\nu_{13}\nu_{31}\right)}{9\pi E_3}r^3\right) \tag{4}$$

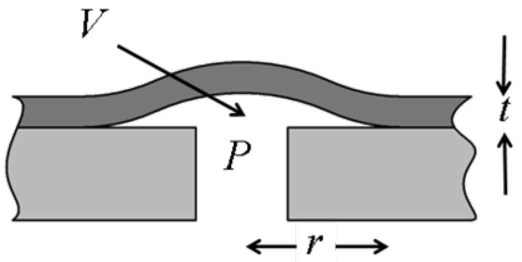

Figure 1. Blister formation of composite repair on top of steel substrate with through hole as artificial corrosion defect

The energy release rate equation consists of three terms, for the bending, the shear and the crack opening displacement (COD).

3 Fracture mechanics for FEA

Two different approaches are used to calculate the energy release rate through finite element analysis. The first one utilizes the above described analytical solution given in Equation (3). But the compliance is replaced with the volume-pressure quotient as given in Equation (5). The required volume for the pressure-volume-method (PVM) is then calculated with FEA.

$$C = V/P \tag{5}$$

$$G = \frac{pdV}{2dA} \tag{6}$$

The other method is the virtual crack closure technique (VCCT). This method is based on the difference in energy between a crack with a crack length *a* and an extended crack length *a+da*. Gaining the released energy in this direct way through the deflection of the nodes allows for the calculation of the energy release rates for all three modes (6) (Fig. 2). A more detailed description of the VCCT can be found in [6].

$$G_I = -\frac{1}{2\Delta A} R_X \Delta u\,; \quad G_{II} = -\frac{1}{2\Delta A} R_Y \Delta v\,; \quad G_{III} = -\frac{1}{2\Delta A} R_Z \Delta w \tag{6}$$

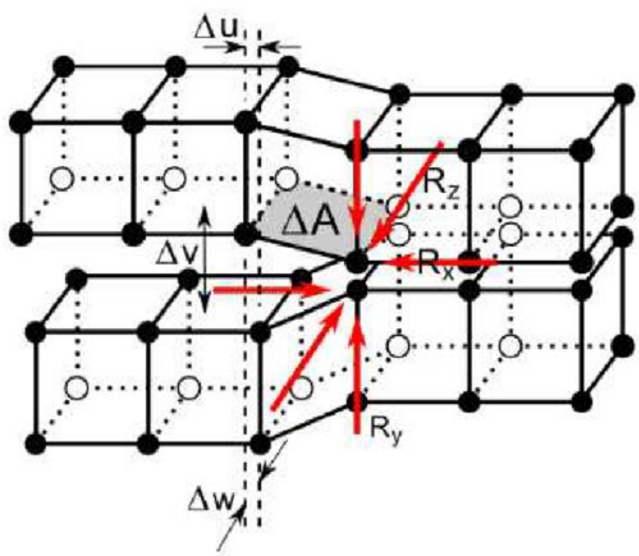

Figure 2. VCCT crack opening; node deflection and force vectors. [5]

Stress intensity factors (SIFs) can be calculated with FEA by the interaction integral method as given in Equation (8). The interaction integral *I* itself is derived from the *J*-integral as shown in Equation (7). Post-processing the results of the displacement, stress and strain, FEA yields the equilibrium state *J* in respect to the particular boundary conditions. Another near-tip auxiliary field J^{aux} is introduced for the determination of the mixed-mode stress intensity factors. Superposing both leads to a third equilibrium state, which is expressed in the total field J^{S}. All combined add up to the interaction integral (8). This method is described amongst other by [7] and [8]. Walters [7] also gives an overview over various integration methods and developments for mixed-mode SIF calculations.

$$I = J^{S} - J - J^{aux} \tag{7}$$

$$I = \frac{-\int_V q_{i,j}\left(\sigma_{kl}\varepsilon_{kl}^{aux}\delta_{ij} - \sigma_{kj}^{aux}u_{k,i} - \sigma_{kj}u_{k,i}^{aux}\right)dV}{\int_s \delta q_n ds} \tag{8}$$

σ, ε, u, q and δ are stress, strain, displacement, crack-extension vector and the Kronecker delta respectively. Values for the auxiliary field are marked with ^{aux}.

The SIFs are connected to the interaction integral via Equation (9).

$$I = \frac{2}{E'}\left[K_I K_I^{aux} + K_{II} K_{II}^{aux}\right] + \frac{1}{G} K_{III} K_{III}^{aux} \tag{9}$$

J-integrals as given in Equation (10) are equal to the energy release rate in the case of linear elastic fracture mechanics, Equation (11) [4] [7]. But the main advantage is that *J*-integrals can also be calculated for inelastic material behaviour [4], in opposite to *G* and *K*.

$$G_C = \int_C \left(W\delta_{li} - \sigma_{ij}u_{j,l}\right)n_i dC \quad \text{with } l, i \text{ running from 1..2, C: contour} \tag{10}$$

$$G = J \tag{11}$$

When applied on 3-D problems the main principle of the briefly above explained equations remains, but the equations themselves become more complex. Discretisation for computing purposes is done by replacing integrals with corresponding summations. Challenging for the implementation in addition to the mathematical programming in a FE analysis is the meshing, since the VCCT needs quadrangles while *J*-integral and SIFs utilize in the crack-tip collapsed meshes.

4 FEA Model

ANSYS WB 13 is used for the FEA simulation. The axi-symmetric model is defined with an infinite stiff substrate and a laminate repair covering a circular through hole with sharp edges. The hole radius is varied from 2.5 mm to 15 mm and the repair thickness between 5 mm and 10 mm. Material parameters can be seen in Table 2.1 and 2.2. It can be seen, that the flexural stiffness of carbon is almost three times as high as glass, while shear is about 6 % higher for glass which is often important for some deflections.

	U/D ply	Q/I laminate	0/90 laminate
E_1 (GPa)	30.2	15.1	19.2
E_2 (GPa)	7.37	15.1	19.2
E_3 (GPa)	7.37	7.37	7.37
G_{12} (GPa)	2.86	6.22	2.86
G_{23} (GPa)	2.59	2.72	2.72
G_{31} (GPa)	2.86	2.72	2.72
ν_{12}	0.303	0.215	0.0021
ν_{31}	0.424	0.173	0.189

Table 2.1 Glass epoxy laminate parameters

	U/D ply	Q/I laminate	0/90 laminate
E_1 (GPa)	98.2	37.3	52.5
E_2 (GPa)	6.22	37.3	52.5
E_3 (GPa)	6.22	6.22	6.22
G_{12} (GPa)	2.73	14.49	2.74
G_{23} (GPa)	2.10	2.42	2.42
G_{31} (GPa)	2.73	2.42	2.42
ν_{12}	0.305	0.289	0.00092
ν_{31}	0.019	0.047	0.019

Table 2.2 Carbon epoxy laminate parameters

	Glass	Carbon
E_1/G_{13}	5.55	15.3
E_3/G_{13}	2.71	2.55

Table 2.3 Ratios of the flexural and shear stiffness

For the calculation of the energy release rate by PVM no special requirements for the simulation apply and a standard simulation (Fig. 3) with focus on deflection, stress and strain was undertaken. The change in volume in the blister was measured and incorporated in the PVM calculation.

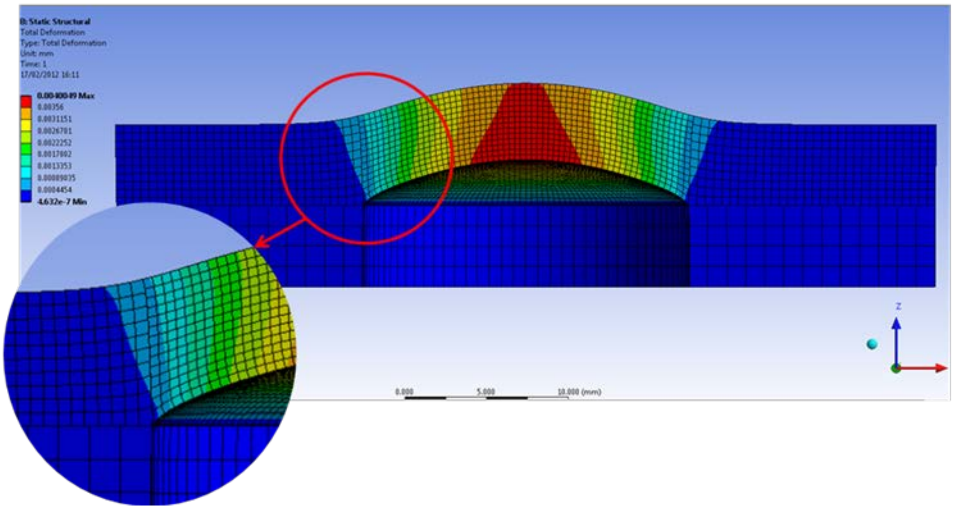

Figure 3. PVM simulation with ANSYS WB 13; Circular zoom illustrates “back span” effect.

Surveying the bending, shear and COD term for themselves provides a better understanding and comparison of analytical model and FEA. Pure bending deflection can be achieved by setting G_{13} and E_3 to high values. Only shear deflection is obtained by putting E_1 and E_3 to high values. G_{13} and E_3 must be high when aiming for the COD deflection. As a fixed support of the laminate at the crack edge is not realistic, no extra boundary conditions are applied for the repair. Hence the strained area is bigger than the defect radius and the formerly vertical nodes show an angle to the outside.

5 Results

Comparing the previous analytical model with the FEA results reveals that both agree reasonably well in the area of low repair aspect ratios (*r/t*) (Fig. 4). Most real repair cases can be found in this area. However the divergence between both curves increases with inclining aspect ratio above 1.5.

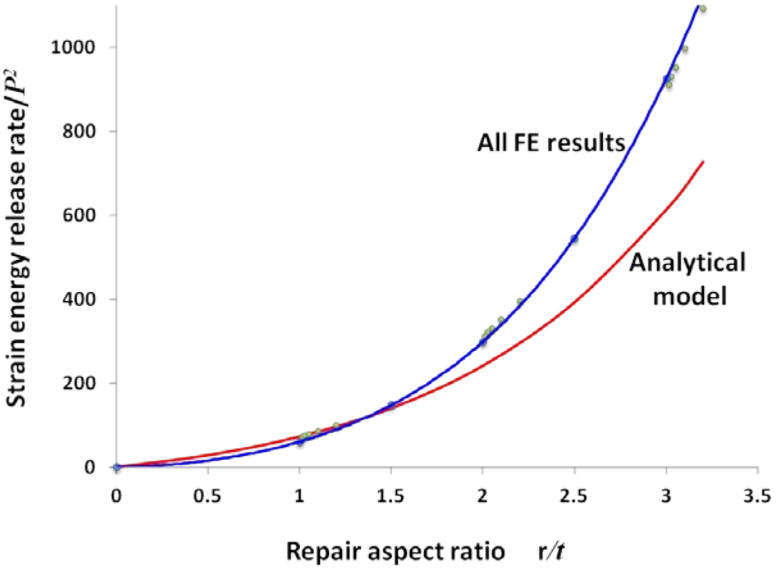

Figure 4. Comparison between previous analytical model and FEA

Figures 5.1-5.3 show the results for pure bending, shear and COD in comparison between FEA and analytical model. It can be seen that the true bending contribution is larger than the analytically gained. The opposite pattern occurs for pure shear. A relative strong difference is shown for the COD. The analytical model results are about seven times larger.

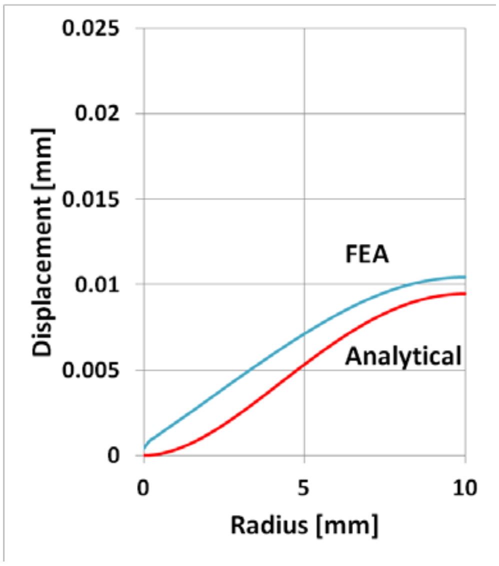

Figure 5.1. Pure bending deflection derived from analytical model and FEA

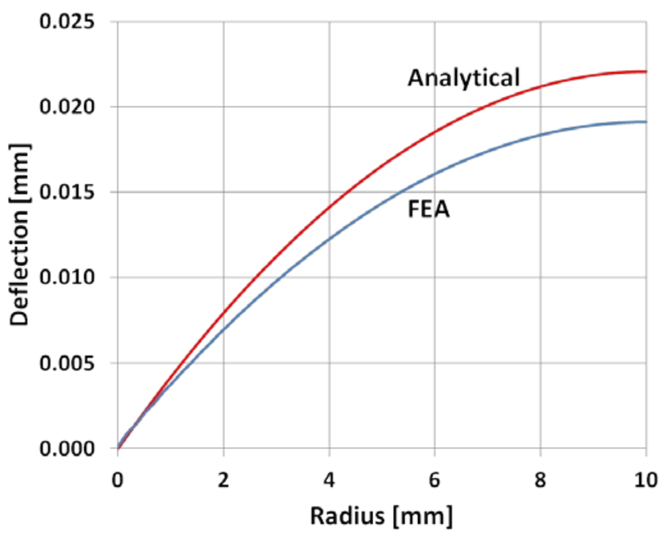

Figure 5.2. Pure shear deflection derived from analytical model and FEA

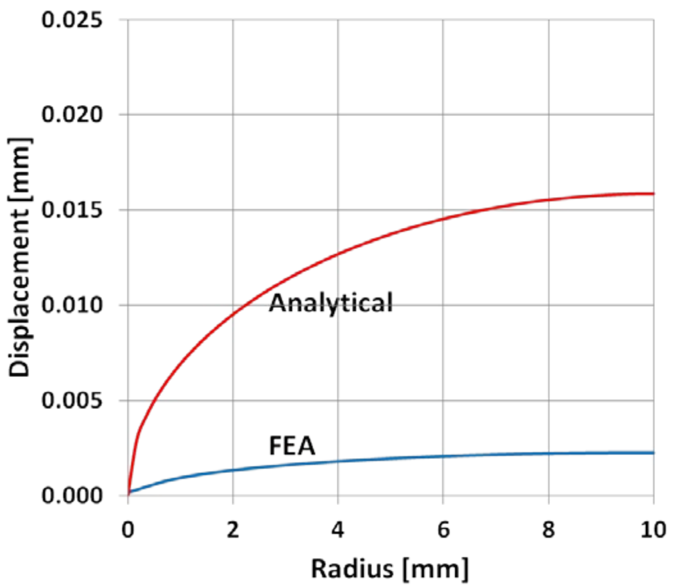

Figure 5.3. Pure crack opening displacement (COD) derived from analytical model and FEA

6 Discussion, conclusions and future work

As seen in Fig. 4, the analytical model used is sufficient for small aspect ratios. However it is possible through a few changes to adjust the model. The change of factors ($k_{1..3}$) for Equation (3) is illustrated in (12). Applying the new constants yields results given in Fig. 6, which shows improved correlation between the FEA and analytical model.

$$G_C = P^2\left(\frac{k_1\left(1-\nu_{12}^2\right)}{E_1 t^3} r^4 + \frac{k_2}{G_{13} t} r^2 + \frac{k_3\left(1-\nu_{13}\nu_{31}\right)}{\pi E_3} r\right) \tag{12}$$

$k_1 = 0.27 \qquad k_2 = 0.17 \qquad k_3 = 1.4$

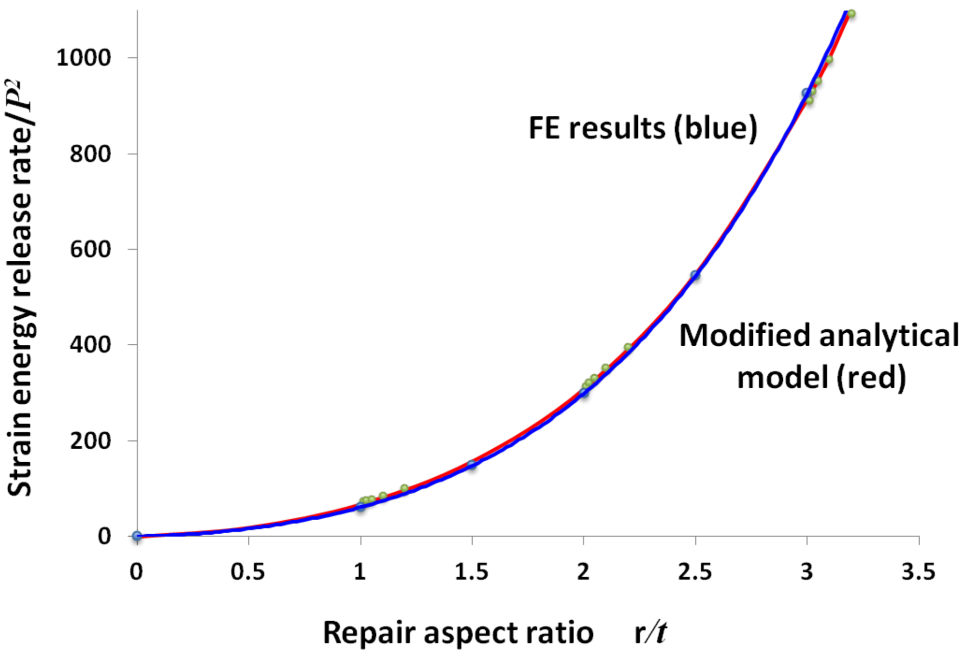

Figure 6. Comparison between improved analytical model and FEA

Standards like the named ISO and ASME make major contribution to the evolving composites engineering in the field of oil and gas in order to make safe and cost-effective repairs. Another refinement for these standards was accomplished in the course of this work. Nevertheless more simulations and tests are necessary and are planned to enhance the understanding and develop applicable tools in form of analytical models for engineers to design repairs.

Acknowledgement
PETRONAS and CRC-ACS are recognised for driving projects in which course this work was done.

References

[1] ISO/TS 24817:2006, *Petroleum and natural gas industries- Composite repairs for pipework- Qualification and testing, installation and inspection*, (2006)
[2] ASME PCC-2, *Repair of pressure vessels and piping*, (2011)
[3] Mableson A. R. et al., "Refurbishment of steel tubular pipes using composite materials", *Plastics, Rubber and Composites*, vol. **29**, no. 10, pp. 558-565, (2000)
[4] Gross D., Seelig Th, *Chapters 4. & 5.* in "Bruchmechanik", Springer, Berlin, 4. Edition, (2007)
[5] ANSYS WB 13, Help file, *12.3 Numerical Evaluation of Fracture Mechanics Parameters*, (2011)
[6] Krüger R., "Virtual crack closure technique: History, approach and applications", *Appl. Mech. Rev.*, vol. **57**, no. 2, (March 2004)
[7] Walters M. C., Paulino G. H., Dodds Jr. R. H., "Interaction integral procedures for 3-D curved cracks including surface tractions", *Eng. Fracture Mech.*, vol. **72**, pp. 1635-1663, (2005)
[8] Gosz M., Moran B., "An interaction energy integral method for computation of mixed-mode stress intensity factors along non-planar crack fronts in three dimensions", *Eng. Fracture Mech.*, vol. **69**, pp. 299-319, (2002)